

Wave Propagation in a Magneto-Micropolar Thermoelastic Medium with Two Temperatures for Three-Phase-Lag Model

Samia M. Said¹

Abstract: The present paper is concerned with the wave propagation in a micropolar thermoelastic solid with distinct two temperatures under the effect of the magnetic field in the presence of the gravity field and an internal heat source. The formulation of the problem is applied in the context of the three-phase-lag model and Green-Naghdi theory without dissipation. The medium is a homogeneous isotropic thermoelastic in the half-space. The exact expressions of the considered variables are obtained by using normal mode analysis. Comparisons are made with the results in the two theories in the absence and presence of the magnetic field as well as the two-temperature parameter. A comparison is also made in the two theories for different values of an internal heat source.

Keywords: Green-Naghdi theory, internal heat source, magnetic field, micropolar, three-phase-lag model, two-temperature.

1 Introduction

The comprehensive review on the micropolar elasticity was given by Eringen (1966, 1970); Nowacki (1986). Chandrasekharaiah (1986) developed a heat flux dependent micropolar thermoelasticity. Kumar and Singh (1998) studied the reflection of plane waves from the flat boundary of a micropolar generalized thermoelastic with stretch. Kumar (2000) investigated the reflection coefficient in a micropolar viscoelastic generalized half-space. Singh (2007) discussed the wave propagation in an orthotropic micropolar elastic solid. A new theory of the generalized thermoelasticity reinforcement has been constructed by taking into account the deformation of a micropolar generalized thermoelastic medium with voids are discussed by Othman, Lotfy, Said, and Anwar Bég (2012). The deformation due to thermo-mechanical sources in a homogeneous isotropic micropolar thermoelastic medium

¹ Department of Mathematics, Faculty of Science, Zagazig University, P.O. Box 44519, Zagazig, Egypt. E-mail: samia_said59@yahoo.com

with void are discussed by Abbas, Kumar, Sharma, and Garg (2015).

The investigation of the interaction between the magnetic field, stress, and strain in a thermoelastic solid is very important due to its many applications in diverse field such as geophysics (for understanding the effect of the Earth's magnetic field on seismic waves), damping of acoustic waves in a magnetic field, designing machine elements like heat exchangers, boiler tubes (where the temperature induced elastic deformation occurs), biomedical engineering (problems involving thermal stress), emissions of the electromagnetic radiations from nuclear devices, development of a highly sensitive super conducting magnetometer, electrical power engineering, plasma physics, etc. Many studies in a generalized magneto-thermoelasticity can be found in the literatures by Youssef (2006); Othman and Kumar (2009); Othman and Atwa (2011); Othman and Abass (2015); Abbas and Zenkour (2015).

A theory of heat conduction in deformable bodies which depends upon two distinct temperatures, the conductive temperature and the thermodynamic temperature, has been established by Chen and Gurtin (1968a); Chen and Williams (1968b); Chen, Gurtin, and Williams (1969). In time-independent problems, the difference between these two distinct temperatures is proportional to the heat supply and in the absence of any heat supply; these two temperatures are identical as Chen and Williams (1968b). In time-dependent situations and of the wave propagation problems, in particular, the two-temperatures are in general different, regardless of the presence of a heat supply. Warren and Chen (1973) have studied the wave propagation in the two-temperature theory of thermoelasticity. Youssef (2005) has proposed a theory in the context of the generalized theory of thermoelasticity with two-temperature. Several problems have been solved by Das and Kanoria (2012); Abbas and Zenkour (2014); Zenkour and Abouelregal (2015) applying the two-temperature theory of thermoelasticity.

It is well known that the usual theory of heat conduction based on Fourier's law predicts an infinite heat propagation speed. It is also known that heat transmission at low temperature propagates by means of waves. These aspects have caused intense activity in the field of heat propagation. Extensive reviews on the second sound theories (hyperbolic heat conduction) are given in Hetnarski and Ignaczak (1999, 2000). A two-phase-lag to both the heat flux vector and the temperature gradient was introduced by Tzou (1995). According to this model, classical Fourier's law $\mathbf{q} = -K\nabla T$ has been replaced by $\mathbf{q}(P, t + \tau_q) = -K\nabla T(P, t + \tau_T)$, where the temperature gradient ∇T at a point P of the material at time $t + \tau_T$ corresponds to the heat flux vector \mathbf{q} at the same point at time $t + \tau_q$. Here K is the thermal conductivity of the material. The delay time τ_T is interpreted as that caused by the micro-structural interactions and is called the phase-lag of the temperature gradient. The other delay time τ_q is interpreted as the relaxation time

due to the fast transient effects of thermal inertia and is called the phase-lag of the heat flux. For $\tau_q = \tau_T = 0$, Fourier's law in a two-phase-lag model is identical with classical Fourier's law. If $\tau_q = \tau$ and $\tau_T = 0$, Tzou (1995) refers to the model as a single-phase-lag model. Recently Choudhuri (2007) has proposed a three-phase-lag (3PHL) thermoelasticity which is able to contain all the previous theories at the same time. In this case Fourier's law $\mathbf{q} = -K\nabla T$ has been replaced by $\mathbf{q}(P, t + \tau_q) = -[K\nabla T(P, t + \tau_T) + K^*\nabla v(P, t + \tau_v)]$, where $\nabla v(\dot{v} = T)$ is the thermal displacement gradient and K^* is the additional material constant and τ_v is the phase-lag for the thermal displacement gradient. The purpose of the work of Choudhuri (2007) is to establish a mathematical model that includes the 3PHL in the heat flux vector, the temperature gradient and in the thermal displacement gradient. For this model, we can consider several kinds of Taylor approximations to recover the previously cited theories. In particular the models of Green and Naghdi (1991, 1992, 1993) are recovered. The introduction of the 3PHL model provides a general theoretical heat conduction model with different micro-structural considerations in order to enable scientists in the field of heat conduction with a multi-scale model to predict accurately the thermal behavior of structures. The three-phase-lag model is very useful in the problems of nuclear boiling, exothermic catalytic reactions, phonon-electron interactions, phonon-scattering, etc. Quintanilla and Racke (2008); Quintanilla (2009); Kar and Kanoria (2009); Kumar, Chawla, and Abbas (2012); Abbas (2014); Kumar and Kumar (2015) have solved different problems applying the 3PHL model.

In the present work, we shall formulate a two-temperature magneto-micropolar thermoelastic problem in the presence of the gravity field for a medium with an internal heat source that is moving with a constant speed. Normal mode analysis is used to obtain the exact expressions for displacement components, force stresses and temperatures. The distributions of the considered variables are given and represented graphically. Comparisons are conducted between the considered variables as calculated from the 3PHL model and Green-Naghdi theory without dissipation (G-N II) in the presence and absence of a magnetic field as well as a two-temperature parameter. A comparison is also made in the two theories for different values of an internal heat source.

2 Formulation of the problem and basic equations

We consider the problem of an isotropic homogeneous micropolar thermoelastic half-space ($x \geq 0$). The generalized thermoelastic medium is permeated into a uniform magnetic field with a constant intensity $\mathbf{H} = (0, H_0, 0)$ which is acting parallel to the y -axis. We are interested in a plane strain in the xz -plane [displacement vector

$$\mathbf{u} = (u, 0, w),] \text{ and } \frac{\partial}{\partial y} = 0.$$

When the z -axis is positive downward the body force components are given by Othman, Elmaklizi, and Said (2013).

$$X = 0, \quad Z = g. \quad (1)$$

The field equations and constitutive relations for a micropolar generalized thermoelastic medium in the absence of body forces and body couples can be written as Eringen (1970), Choudhuri (2007) and Youssef (2005) in the context of generalized thermoelasticity as follows:

The constitutive law of the theory of generalized thermoelasticity is

$$\sigma_{ij} = \lambda e_{kk} \delta_{ij} + 2\mu e_{ij} + k u_{j,i} - k \Phi_r \varepsilon_{ijr} - \gamma \hat{T} \delta_{ij}, \quad e_{kk} = \nabla \cdot \underline{u} = \frac{\partial u}{\partial x} + \frac{\partial w}{\partial z}, \quad (2)$$

where σ_{ij} are the components of stress, e_{ij} are the components of strain, e_{kk} is the dilatation, λ, μ are the elastic constants, $\gamma = (3\lambda + 2\mu)\alpha_t$, α_t is the thermal expansion coefficient, $\hat{T} = T - T_0$, where T is the temperature above the reference temperature T_0 , ε_{ijr} is the alternate tensor and δ_{ij} is the Kronecker delta. The strains can be expressed in terms of the displacement u_i as

$$e_{ij} = \frac{1}{2}(u_{i,j} + u_{j,i}), \quad i \cdot j = x, z. \quad (3)$$

We restrict our analysis parallel to the xz -plane with the micro-rotation vector $\boldsymbol{\phi} = (0, \Phi_2, 0)$. In the above equations a comma followed by a suffix denotes partial derivative with respect to the corresponding coordinates.

Eq. (2), then yields

$$\sigma_{xx} = A_1 \frac{\partial u}{\partial x} + \lambda \frac{\partial w}{\partial z} - \gamma \hat{T}, \quad (4)$$

$$\sigma_{zz} = \lambda \frac{\partial u}{\partial x} + A_1 \frac{\partial w}{\partial z} - \gamma \hat{T}, \quad (5)$$

$$\sigma_{xz} = \mu \frac{\partial u}{\partial z} + (\mu + k) \frac{\partial w}{\partial x} + k \Phi_2, \quad \sigma_{zx} = (\mu + k) \frac{\partial u}{\partial z} + \mu \frac{\partial w}{\partial x} - k \Phi_2, \quad (6)$$

where $A_1 = \lambda + 2\mu + k$.

2.1 Equation of motion:

$$\rho \frac{\partial^2 u}{\partial t^2} = \frac{\partial \sigma_{xx}}{\partial x} + \frac{\partial \sigma_{xz}}{\partial z} + \rho g \frac{\partial w}{\partial x} + F_1, \quad (7)$$

$$\rho \frac{\partial^2 w}{\partial t^2} = \frac{\partial \sigma_{zx}}{\partial x} + \frac{\partial \sigma_{zz}}{\partial z} - \rho g \frac{\partial u}{\partial x} + F_3, \quad (8)$$

where F_1, F_3 are the Lorentz force and are given in the form,

$$F_i = \mu_0 (\mathbf{J} \wedge \mathbf{H})_i. \quad (9)$$

The variations of the magnetic and electric fields are perfectly conducting slowly moving medium and are given by Maxwell's equation as Othman and Atwa (2011).

$$\mathbf{J} = \nabla \wedge \mathbf{h} - \epsilon_0 \frac{\partial \mathbf{E}}{\partial t}, \quad (10)$$

$$\nabla \wedge \mathbf{E} = -\mu_0 \frac{\partial \mathbf{h}}{\partial t}, \quad (11)$$

$$\mathbf{E} = -\mu_0 (\dot{\mathbf{u}} \wedge \mathbf{H}), \quad (12)$$

$$\nabla \cdot \mathbf{h} = 0, \quad (13)$$

where μ_0 is the magnetic permeability, ϵ_0 is the electric permeability, \mathbf{J} is the current density vector, $\dot{\mathbf{u}}$ is the particle velocity of the medium, and the small effect of the temperature gradient on \mathbf{J} is also ignored. The dynamic displacement vector is actually measured from a steady-state deformed position and the deformation is assumed to be small. Due to the application of the initial magnetic field \mathbf{H} there are an induced magnetic field $\mathbf{h} = (0, h, 0)$ and an induced electric field \mathbf{E} , as well as the simplified equations of electrodynamics of a slowly moving medium for a homogeneous, thermal and electrically conducting, elastic solid. Expressing the vector \mathbf{J} in terms of the displacement by eliminating the quantities \mathbf{h} and \mathbf{E} from Eq. (10), thus yields,

$$\mathbf{J} = \left(-\frac{\partial h}{\partial z} - \mu_0 \epsilon_0 H_0 \frac{\partial^2 w}{\partial t^2}, 0, \frac{\partial h}{\partial x} + \mu_0 \epsilon_0 H_0 \frac{\partial^2 u}{\partial t^2} \right) \quad (14)$$

Substituting Eq. (14) into Eq. (9), we get

$$F_1 = -\mu_0 H_0 \frac{\partial h}{\partial x} - \epsilon_0 \mu_0^2 H_0^2 \frac{\partial^2 u}{\partial t^2}, \quad F_2 = 0, \quad F_3 = -\mu_0 H_0 \frac{\partial h}{\partial z} - \epsilon_0 \mu_0^2 H_0^2 \frac{\partial^2 w}{\partial t^2}. \quad (15)$$

2.2 Heat conduction equation

$$K^* \nabla^2 \Phi + \tau_v^* \nabla^2 \dot{\Phi} + K_1 \tau_T \nabla^2 \ddot{\Phi} = \left(1 + \tau_q \frac{\partial}{\partial t} + \frac{1}{2} \tau_q^2 \frac{\partial^2}{\partial t^2} \right) (\rho C_E \dot{T} + \gamma T_0 \ddot{e} - Q), \quad (16)$$

The relation between the conductive temperature and the thermodynamics temperature is

$$\Phi - T = \delta \Phi_{,ii}, \quad (17)$$

where K^* is the additional material constant, K_1 is the coefficient of thermal conductivity, ρ is the mass density, C_E is the specific heat at constant strain, Q is a moving internal heat source, τ_T and τ_q are the phase-lag of temperature gradient and the phase-lag of heat flux respectively. Also $\tau_v^* = K + \tau_v K^*$, where τ_v is the phase-lag of thermal displacement gradient.

2.3 The equations of micropolar materials

$$(\alpha + \beta + \gamma_1)\nabla(\nabla \cdot \boldsymbol{\phi}) - \gamma_1 \nabla \wedge (\nabla \wedge \boldsymbol{\phi}) + k(\nabla \wedge \mathbf{u}) - 2k\boldsymbol{\phi} = \rho J_0 \frac{\partial^2 \boldsymbol{\phi}}{\partial t^2}, \quad (18)$$

$$m_{ij} = \alpha \Phi_{r,r} \delta_{ij} + \beta \Phi_{i,j} + \gamma_1 \Phi_{j,i}, \quad (19)$$

Where $\alpha, \beta, \gamma_1, k$ are the material constants. J_0 is micro-inertia and m_{ij} is the couple stress tensor.

Introducing Eqs. (4)–(6) and (15) in Eqs. (7), (8) we get

$$\begin{aligned} \rho \frac{\partial^2 u}{\partial t^2} = & A_1 \frac{\partial^2 u}{\partial x^2} + A_2 \frac{\partial^2 w}{\partial x \partial z} + \mu \frac{\partial^2 u}{\partial z^2} - \gamma \frac{\partial \hat{T}}{\partial x} + k \frac{\partial \Phi_2}{\partial z} \\ & + \rho g \frac{\partial w}{\partial x} - \mu_0 H_0 \frac{\partial h}{\partial x} - \varepsilon_0 \mu_0^2 H_0^2 \frac{\partial^2 u}{\partial t^2}, \end{aligned} \quad (20)$$

$$\begin{aligned} \rho \frac{\partial^2 w}{\partial t^2} = & \mu \frac{\partial^2 w}{\partial x^2} + A_2 \frac{\partial^2 u}{\partial x \partial z} + A_1 \frac{\partial^2 w}{\partial z^2} - \gamma \frac{\partial \hat{T}}{\partial z} - k \frac{\partial \Phi_2}{\partial x} \\ & - \rho g \frac{\partial u}{\partial x} - \mu_0 H_0 \frac{\partial h}{\partial z} - \varepsilon_0 \mu_0^2 H_0^2 \frac{\partial^2 w}{\partial t^2}, \end{aligned} \quad (21)$$

where $A_2 = \lambda + \mu + k$.

Using $h = -H_0 e$, then introducing the following non-dimension quantities in the above equation (dropping the primes for convenience):

$$\begin{aligned} (x', z', u', w') = & c_1 \eta (x, z, u, w), \quad (t', \tau'_q, \tau'_v, \tau'_T) = c_1^2 \eta (t, \tau_q, \tau_v, \tau_T), \quad g' = \frac{\rho g}{A_1 c_1 \eta}, \\ \theta = & \frac{\gamma \hat{T}}{A_1}, \quad \Phi' = \frac{\gamma(\Phi - T_0)}{A_1}, \quad Q' = \frac{\gamma}{\rho C_E c_1^4 \eta^2 A_1} Q, \quad \sigma'_{ij} = \frac{\sigma_{ij}}{\mu}, \quad \Phi'_2 = \Phi_2, \\ m'_{ij} = & \frac{\eta}{\rho c_1} m_{ij}, \quad i, j = 1, 2. \end{aligned} \quad (22)$$

Where $\eta = \frac{\rho C_E}{K^*}$, $c_1^2 = \frac{A_1}{\rho}$.

Thus we get,

$$\alpha_1 \frac{\partial^2 u}{\partial t'^2} = \frac{\partial^2 u}{\partial x'^2} + \frac{A_2}{A_1} \frac{\partial^2 w}{\partial x' \partial z'} + \frac{\mu}{A_1} \frac{\partial^2 u}{\partial z'^2} - \frac{\partial \theta}{\partial x'} + \frac{k}{A_1} \frac{\partial \Phi_2}{\partial z'} + g' \frac{\partial w}{\partial x'} + R_H \frac{\partial e}{\partial x'}, \quad (23)$$

$$\alpha_1 \frac{\partial^2 w}{\partial t^2} = \frac{\partial^2 w}{\partial z^2} + \frac{A_2}{A_1} \frac{\partial^2 u}{\partial x \partial z} + \frac{\mu}{A_1} \frac{\partial^2 w}{\partial x^2} - \frac{\partial \theta}{\partial z} - \frac{k}{A_1} \frac{\partial \Phi_2}{\partial x} - g \frac{\partial u}{\partial x} + R_H \frac{\partial e}{\partial z}, \quad (24)$$

$$\nabla^2 \Phi_2 + B_1 \left(\frac{\partial u}{\partial z} - \frac{\partial w}{\partial x} \right) - 2B_1 \Phi_2 = B_2 \frac{\partial^2 \Phi_2}{\partial t^2}, \quad (25)$$

$$C_K \Phi_{,ii} + C_V \dot{\Phi}_{,ii} + C_T \ddot{\Phi}_{,ii} = \left(1 + \tau_q \frac{\partial}{\partial t} + \frac{1}{2} \tau_q^2 \frac{\partial^2}{\partial t^2} \right) (\ddot{\theta} + \varepsilon \ddot{e} - Q), \quad (26)$$

$$\Phi - \theta = \beta_0 \Phi_{,ii}, \quad (27)$$

where,

$$\alpha_1 = \frac{(\rho + \varepsilon_0 \mu_0^2 H_0^2) c_1^2}{A_1}, \quad R_H = \frac{\mu_0 H_0^2}{A_1}, \quad B_1 = \frac{K}{\gamma_1 c_1^2 \eta^2}, \quad B_2 = \frac{\rho J_0 c_1^2}{\gamma_1}, \quad C_K = \frac{K^*}{\rho C_E c_1^2},$$

$$C_V = \frac{\eta K_1}{\rho C_E} + C_K \tau_v, \quad C_T = \frac{\eta K_1 \tau_T}{\rho C_E}, \quad \varepsilon = \frac{\gamma^2 T_0}{\rho C_E A_1}, \quad \beta_0 = \delta c_1^2 \eta^2.$$

Introducing potential functions defined by

$$u = \frac{\partial q}{\partial x} + \frac{\partial \psi}{\partial z}, \quad w = \frac{\partial q}{\partial z} - \frac{\partial \psi}{\partial x}. \quad (28)$$

where $q(x, z, t)$, and $\psi(x, z, t)$, are scalar potential functions.

Introducing Eq. (28) in Eqs. (23)–(26), we get

$$\alpha_1 \frac{\partial^2 q}{\partial t^2} = R_1 \nabla^2 q - \theta - g \frac{\partial \psi}{\partial x}, \quad (29)$$

$$\alpha_1 \frac{\partial^2 \psi}{\partial t^2} = \frac{\mu}{A_1} \nabla^2 \psi + \frac{k}{A_1} \Phi_2 + g \frac{\partial q}{\partial x}, \quad (30)$$

$$B_2 \frac{\partial^2 \Phi_2}{\partial t^2} = (\nabla^2 - 2B_1) \Phi_2 + B_1 \nabla^2 \psi, \quad (31)$$

$$C_K \Phi_{,ii} + C_V \dot{\Phi}_{,ii} + C_T \ddot{\Phi}_{,ii} = \left(1 + \tau_q \frac{\partial}{\partial t} + \frac{1}{2} \tau_q^2 \frac{\partial^2}{\partial t^2} \right) (\ddot{\theta} + \varepsilon \nabla^2 \ddot{q} - Q), \quad (32)$$

Where $R_1 = 1 + R_H$.

3 Normal mode analysis

The solution of the considered physical variable can be decomposed in terms of normal modes as the following form:

$$\begin{aligned} & [u, w, q, \psi, \theta, \Phi_2, \Phi, \sigma_{ij}, m_{ij}](x, z, t) \\ & = [u^*, w^*, q^*, \psi^*, \theta^*, \Phi_2^*, \Phi^*, \sigma_{ij}^*, m_{ij}^*](z) \exp(mt + iax), \end{aligned}$$

$$Q = Q^* \exp(mt + iax), \quad Q^* = Q_0 v_0, \quad (33)$$

where m is a complex constant, $i = \sqrt{-1}$, a is the wave number in the x -direction, v_0 is the velocity of a moving internal heat source, Q_0 is the magnitude of an internal heat source and $u^*(x), w^*(x), q^*(x), \psi^*(x), \theta^*(x), \Phi_2^*(x), \Phi^*(x), \sigma_{ij}^*(x), m_{ij}^*(x)$ are the amplitudes of the field quantities.

Introducing Eqs. (33) in Eqs. (29)–(32) and Eq. (27), we obtain

$$[R_1 D^2 - N_1] q^* - iag \psi^* = (N_9 - \beta_0 D^2) \Phi^*, \quad (34)$$

$$[N_2 D^2 - N_3] \psi^* + iag q^* + k_A \Phi_2^* = 0, \quad (35)$$

$$[D^2 - N_4] \Phi_2^* + [B_1 D^2 - B_1 a^2] \psi^* = 0, \quad (36)$$

$$[\varepsilon N_5 D^2 - N_6] q^* = [N_{10} D^2 - N_{11}] \Phi^* + N_0 Q_0 v_0, \quad (37)$$

$$\theta^* = (N_9 - \beta_0 D^2) \Phi^*, \quad (38)$$

where

$$\begin{aligned} N_0 &= 1 + \tau_q m + \frac{1}{2} \tau_q^2 m^2, \quad N_1 = R_1 a^2 + \alpha_1 m^2, \quad N_2 = \frac{\mu}{A_1}, \quad N_3 = N_2 a^2 + \alpha_1 m^2, \\ N_4 &= a^2 + 2B_1 + B_2 m^2, \quad N_5 = m^2 N_0, \quad N_6 = \varepsilon a^2 N_5, \quad N_7 = C_K + C_v m + C_T m^2, \\ N_8 &= a^2 N_7, \quad N_9 = 1 + \beta_0 a^2, \quad N_{10} = \beta_0 N_5 + N_7, \quad N_{11} = N_5 N_9 + N_8, \\ k_A &= \frac{k}{A_1}, \quad D = \frac{d}{dx}. \end{aligned}$$

Eliminating $\psi^*(x), \Phi_2^*(x)$ and $\theta^*(x)$ between Eqs. (34)–(37), we obtain the eighth-order ordinary differential equation satisfied with $q^*(x)$,

$$[D^8 - S_1 D^6 + S_2 D^4 - S_3 D^2 + S_4] q^*(x) = \frac{-N_0 N_9 Q_0 v_0 (N_3 N_4 + B_1 a^2 k_A)}{L_0}, \quad (39)$$

$$\text{where, } S_1 = \frac{L_1}{L_0}, \quad S_2 = \frac{L_2}{L_0}, \quad S_3 = \frac{L_3}{L_0}, \quad S_4 = \frac{L_4}{L_0}, \quad L_0 = (R_1 N_{10} + \varepsilon N_5 \beta_0) N_2,$$

$$\begin{aligned} L_1 &= R_1 N_{10} N_3 + \varepsilon N_5 N_3 \beta_0 + R_1 N_2 N_4 N_{10} + \varepsilon \beta_0 N_5 N_2 N_4 + R_1 N_{10} B_1 k_A + \varepsilon \beta_0 N_5 B_1 k_A \\ &\quad + N_1 N_2 N_{10} + N_2 N_{11} R_1 + \varepsilon N_2 N_5 N_9 + N_2 N_6 \beta_0, \end{aligned}$$

$$\begin{aligned} L_2 &= -a^2 g^2 N_{10} + R_1 N_3 N_4 N_{10} + \varepsilon \beta_0 N_3 N_4 N_5 + R_1 k_A a^2 B_1 N_{10} + \varepsilon \beta_0 a^2 k_A N_5 \\ &\quad + N_1 N_3 N_{10} + N_3 N_{11} R_1 + \varepsilon N_3 N_5 N_9 + N_3 N_6 \beta_0 + N_1 N_2 N_4 N_{10} + N_2 N_4 N_{11} R_1 \\ &\quad + \varepsilon N_2 N_4 N_5 N_9 + \beta_0 N_2 N_4 N_6 + B_1 k_A N_1 N_{10} + B_1 k_A N_{11} R_1 + \varepsilon N_5 N_9 B_1 k_A \\ &\quad + B_1 k_A \beta_0 N_6 + N_1 N_2 N_{11} + N_2 N_6 N_9, \end{aligned}$$

$$L_3 = -a^2 g^2 N_{11} - a^2 g^2 N_4 N_{10} + N_1 N_3 N_4 N_{10} + N_3 N_4 N_{11} R_1 + \varepsilon N_3 N_4 N_5 N_9$$

$$\begin{aligned}
& + \beta_0 N_3 N_4 N_6 + N_1 N_{10} B_1 a^2 k_A + N_{11} R_1 B_1 a^2 k_A + \epsilon N_5 N_9 B_1 a^2 k_A + \beta_0 B_1 a^2 k_A N_6 \\
& + N_1 N_3 N_{11} + N_3 N_6 N_9 + N_1 N_2 N_4 N_{11} + N_2 N_4 N_6 N_9 + N_1 N_{11} B_1 k_A + N_6 N_9 B_1 k_A, \\
L_4 = & -a^2 g^2 N_4 N_{11} + N_1 N_3 N_4 N_{11} + N_3 N_4 N_6 N_9 + N_1 N_{11} B_1 a^2 k_A + N_6 N_9 B_1 a^2 k_A.
\end{aligned}$$

Equation (39) can be factored as

$$(D^2 - k_1^2) (D^2 - k_2^2) (D^2 - k_3^2) (D^2 - k_4^2) q^*(x) = \frac{-N_0 N_9 Q_0 v_0 (N_3 N_4 + B_1 a^2 k_A)}{L_0}, \quad (40)$$

where $k_n^2 (n = 1, 2, 3, 4)$ are the roots of the following characteristic equation:

$$k^8 - S_1 k^6 + S_2 k^4 - S_3 k^2 + S_4 = 0. \quad (41)$$

The solution of Eq. (39), which is bound as $x \rightarrow \infty$, is given by

$$q^*(x) = \sum_{n=1}^4 M_n \exp(-k_n z) - \frac{N_0 N_9 Q_0 v_0 (N_3 N_4 + B_1 a^2 k_A)}{L_0 S_4}. \quad (42)$$

In a similar manner, we get that

$$\psi^*(x) = \sum_{n=1}^4 H_{1n} M_n \exp(-k_n z) - \frac{i a g N_0 N_4 N_9 Q_0 v_0}{S_4 L_0}. \quad (43)$$

$$\Phi^*(x) = \sum_{n=1}^4 H_{2n} M_n \exp(-k_n z) + \frac{N_0 Q_0 v_0 (N_1 N_3 N_4 + N_1 B_1 k_A a^2 - a^2 g^2 N_4)}{S_4 L_0}. \quad (44)$$

$$\Phi_2^*(x) = \sum_{n=1}^4 H_{3n} M_n \exp(-k_n z) + \frac{i a^3 g B_1 N_0 N_9 Q_0 v_0}{S_4 L_0}. \quad (45)$$

where M_n are parameters,

$$\begin{aligned}
H_{1n} &= \frac{i a g (N_4 - k_n^2)}{N_2 k_n^4 - (N_3 + N_2 N_4 + B_1 k_A) k_n^2 + N_3 N_4 + B_1 a^2 k_A}, \\
H_{2n} &= \frac{R_1 k_n^2 - N_1 - i a g H_{1n}}{N_9 - \beta_0 k_n}, \quad H_{3n} = \frac{(N_2 k_n^2 - N_3) H_{1n} + i a g}{-k_A}.
\end{aligned}$$

Introducing Eq. (44) in Eq. (38), this yields

$$\theta^*(x) = \sum_{n=1}^4 H_{4n} M_n \exp(-k_n z) + \frac{N_0 N_9 Q_0 v_0 (N_1 N_3 N_4 + N_1 B_1 k_A a^2 - a^2 g^2 N_4)}{S_4 L_0}. \quad (46)$$

where, $H_{4n} = (N_9 - \beta_0 k_n^2) H_{2n}$.

Introducing Eq. (42) and (43) in Eq. (28), this yields

$$u^*(x) = \sum_{n=1}^4 H_{5n} M_n \exp(-k_n z) - \frac{iaN_0 N_9 Q_0 v_0 (N_3 N_4 + B_1 a^2 k_A)}{L_0 S_4}. \quad (47)$$

$$w^*(x) = \sum_{n=1}^4 H_{6n} M_n \exp(-k_n z) - \frac{a^2 g N_0 N_4 N_9 Q_0 v_0}{S_4 L_0}. \quad (48)$$

where, $H_{5n} = ia - H_{1n} k_n$, $H_{6n} = -k_n - ia H_{1n}$.

Introducing Eqs. (22) and (33) in Eqs. (5) and (6), we get

$$\mu \sigma_{zz}^* = ia \lambda u^* + A_1 D w^* - A_1 \theta^*, \quad (49)$$

$$\mu \sigma_{xz}^* = \mu D u^* + ia(\mu + k) w^* + k \Phi_2^*. \quad (50)$$

Introducing Eqs. (45)–(48) in Eqs. (49) and (50), this yields

$$\sigma_{zz}^* = \sum_{n=1}^4 H_{7n} M_n \exp(-k_n z) + r_1, \quad (51)$$

$$\sigma_{xz}^* = \sum_{n=1}^4 H_{8n} M_n \exp(-k_n z) + r_2, \quad (52)$$

where,

$$H_{7n} = \frac{1}{\mu} [ia \lambda H_{5n} - A_1 H_{6n} k_n - A_1 H_{4n}], \quad H_{8n} = \frac{1}{\mu} [-\mu H_{5n} k_n + ia(\mu + k) H_{6n} + k H_{3n}],$$

$$r_1 = \frac{N_0 N_9 Q_0 v_0 [\lambda a^2 (N_3 N_4 + B_1 a^2 k_A) - A_1 (N_1 N_3 N_4 + N_1 B_1 a^2 k_A - a^2 g^2 N_4)]}{\mu S_4 L_0},$$

$$r_2 = \frac{ia^3 g N_0 N_9 Q_0 v_0 [k B_1 - (\mu + k) N_4]}{\mu S_4 L_0}.$$

From Eqs. (22) and (33) in Eqs. (19), we get

$$m_{zy}^* = \frac{\gamma \eta^2}{\rho} D \Phi_2^* \quad (53)$$

Introducing Eqs. (45) in Eqs. (53), this yields

$$m_{zy}^* = \sum_{n=1}^4 H_{9n} M_n \exp(-k_n z), \quad (54)$$

where $H_{9n} = -\frac{\gamma \eta^2}{\rho} k_n H_{3n}$.

4 Application

We consider a generalized two-temperature magneto-micropolar thermoelastic problem for a medium with an internal heat source that is moving with a constant speed in the presence of the gravity field which fills the region Ω defined as follows:

$$\Omega = \{(x, y, z) : 0 \leq x < \infty, -\infty < y < \infty, -\infty < z < \infty\}.$$

In the physical problem, we should suppress the positive exponentials that are unbounded at infinity. The constants M_n ($n = 1, 2, 3, 4$) have to be chosen such that the boundary conditions on the surface at $z = 0$ are as follows:

$$\sigma_{zz} = -f(x, t) = -f^* \exp(mt + iax) \quad \Phi = \sigma_{xz} = m_{zy} = 0. \quad (55)$$

Where, $f(x, t)$ is an arbitrary function of x, t , and f^* is the magnitude of the mechanical force. Using the expressions of the variables considered into the above boundary conditions (Eqs. (55)), we can obtain the following equations satisfied with the parameters:

$$\sum_{n=1}^3 H_{2n} M_n = -R_0, \quad (56)$$

$$\sum_{n=1}^3 H_{7n} M_n = -f^* - r_1, \quad (57)$$

$$\sum_{n=1}^3 H_{8n} M_n = -r_2, \quad (58)$$

$$\sum_{n=1}^3 H_{9n} M_n = 0, \quad (59)$$

$$\text{where, } R_0 = \frac{N_0 Q_0 \nu_0 (N_1 N_3 N_4 + N_1 B_1 k_A a^2 - a^2 g^2 N_4)}{S_4 L_0}.$$

Invoking Eqs. (56)–(59), we obtain a system of four equations. After applying the inverse of matrix method, we have the values of the four constants M_n ($n = 1, 2, 3, 4$). Hence, we obtain the expressions of the considered variables.

$$\begin{pmatrix} M_1 \\ M_2 \\ M_3 \\ M_4 \end{pmatrix} = \begin{pmatrix} H_{21} & H_{22} & H_{23} & H_{24} \\ H_{71} & H_{72} & H_{73} & H_{74} \\ H_{81} & H_{82} & H_{83} & H_{84} \\ H_{91} & H_{92} & H_{93} & H_{94} \end{pmatrix}^{-1} \begin{pmatrix} -R_0 \\ -f^* - r_1 \\ -r_2 \\ 0 \end{pmatrix} \quad (60)$$

5 Particular cases and special cases of thermoelastic theory

- i. The corresponding equations for a two-temperature micropolar thermoelastic medium with an internal heat source ($Q_0 = 5.5$) in the presence of the gravity field from the above mentioned cases by taking H_0 to vanish.
- ii. The corresponding equations for a magneto-micropolar thermoelastic medium with an internal heat source ($Q_0 = 5.5$) in the presence of the gravity field from the above mentioned cases by taking δ to vanish.
- iii. The corresponding equations for a two-temperature magneto-micropolar thermoelastic medium in the presence of the gravity field for different values of an internal heat source from the above mentioned cases by taking $Q_0 = 5.5, 1$.
- iv. Equations of the 3PHL model when $K, \tau_T, \tau_q, \tau_v > 0$ and the solutions are always (exponentially) stable if $\frac{2K\tau_T}{\tau_q} > \tau_v^* > K^*\tau_q$ as in Quintanilla and Racke (2008).
- v. Equations of the G-N II theory when $K = \tau_T = \tau_q = \tau_v = 0$.

6 Numerical calculation and discussion

In order to illustrate the theoretical results obtained in the preceding section, and to compare these in the context of the 3PHL model and the GN-II theory, we now present some numerical results for the physical constants as

$$\begin{aligned} \lambda &= 7.76 \times 10^{10} \text{ N} \cdot \text{m}^{-2}, \quad \mu = 7.86 \times 10^{10} \text{ N} \cdot \text{m}^{-2}, \quad \rho = 8954 \text{ kg} \cdot \text{m}^{-3}, \quad a = 0.1, \\ C_E &= 383.1 \text{ J} \cdot \text{kg}^{-1} \cdot \text{K}^{-1}, \quad f^* = 1.2, \quad \tau_T = 7 \times 10^{-7} \text{ s}, \quad \tau_q = 9 \times 10^{-7} \text{ s}, \\ \tau_v &= 6 \times 10^{-7} \text{ s}, \quad \alpha_l = 1.78 \times 10^{-4} \text{ K}^{-1}, \quad K^* = 386 \text{ w} \cdot \text{m}^{-1} \cdot \text{K}^{-1} \cdot \text{s}^{-1}, \\ v_0 &= 0.4 \text{ m} \cdot \text{s}^{-1}, \quad T_0 = 293 \text{ K}, \quad \mu_0 = 1.9, \quad \varepsilon_0 = 0.7, \quad K_1 = 150 \text{ w} \cdot \text{m}^{-1} \cdot \text{K}^{-1}, \\ m &= m_0 + i\xi, \quad \xi = -0.7, \quad m_0 = 0.3, \quad k = 0.5 \text{ N} \cdot \text{m}^{-2}, \quad J_0 = 2 \times 10^{-12} \text{ N} \cdot \text{m} \cdot \text{kg}^{-1}, \\ g &= 9.8 \text{ m} \cdot \text{s}^{-2}, \quad \delta = 2 \times 10^{-14}, \quad \gamma_1 = 0.0779 \text{ N} \cdot \text{m}^{-2}. \end{aligned}$$

The computations were carried out for a value of time $t = 1.2$. The vertical displacement component w , the thermodynamic temperature θ , the conductive temperature Φ , the stress components σ_{zz}, σ_{xz} , the tangential couple stress m_{zy} and micro-rotation component Φ_2 with distance z for the value of x , namely $x = 1.5$, were substituted in performing the computations. The results are shown in figures

1–21. The graphs show the four curves predicted by two different theories of thermoelasticity. In these figures, the solid lines represent the solution in the 3PHL model, and the dashed lines represent the solution derived using the G-N II theory.

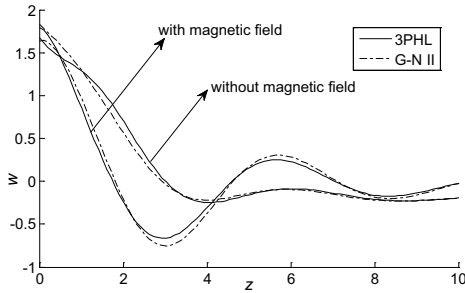


Figure 1: Vertical displacement distribution w in the absence and presence of a magnetic field.

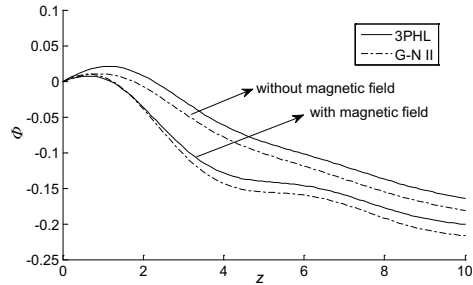


Figure 2: Conductive temperature distribution Φ in the absence and presence of a magnetic field.

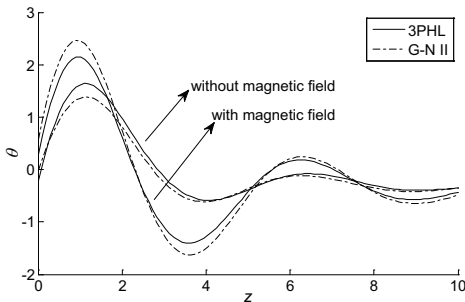


Figure 3: Thermodynamic temperature distribution θ in the absence and presence of a magnetic field.

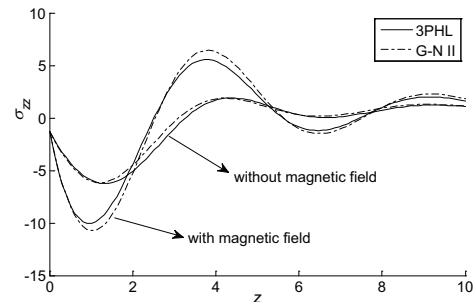


Figure 4: Distribution of the stress component σ_{zz} in the absence and presence of a magnetic field.

Figures 1–7 show comparisons between the vertical displacement w , the thermodynamic temperature θ , the conductive temperature Φ , the stress components σ_{zz} , σ_{xz} , the tangential couple stress m_{zy} and micro-rotation component Φ_2 in the absence ($H_0 = 0$) and presence ($H_0 = 140$) of a magnetic field with a two-temperature parameter ($\delta = 2 \times 10^{-14}$) and an internal heat source ($Q_0 = 5.5$).

Figure 1 depicts that the distribution of the vertical displacement w begins from positive values. In the context of the two theories and in the presence of a magnetic field, w starts with decreasing to a minimum value, then increases, and also moves in the wave propagation. However, in the context of the two theories and in

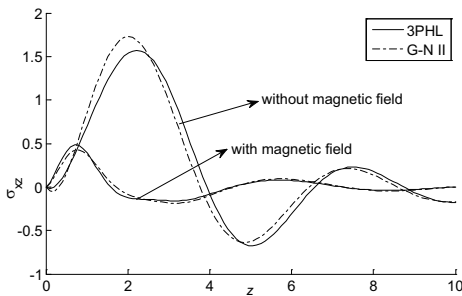


Figure 5: Distribution of the stress component σ_{xz} in the absence and presence of a magnetic field.

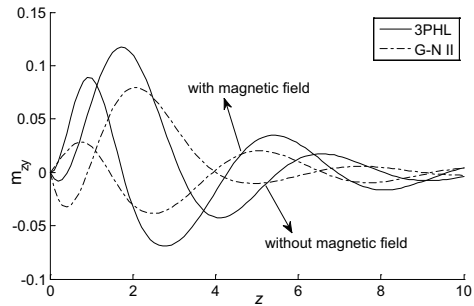


Figure 6: Distribution of the tangential couple stress m_{zy} in the absence and presence of a magnetic field.

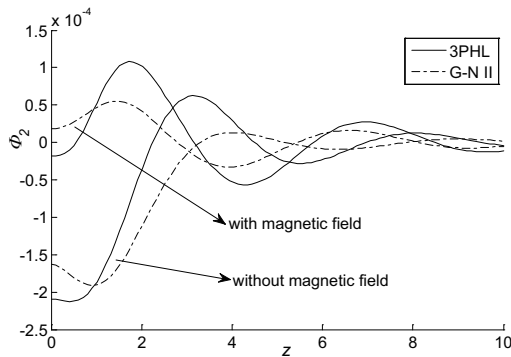


Figure 7: Distribution of the micro-rotation component Φ_2 in the absence and presence of a magnetic field.

the absence of a magnetic field, w starts with decreasing, then increases, after then becomes nearly constant. The magnetic field decreases the magnitude of w then increases it. Figure 2 exhibits the distribution of the conductive temperature Φ and demonstrates that it reaches a zero value and satisfies the boundary condition at $x = 0$. In the context of the two theories, in the absence and presence of a magnetic field, Φ decreases in the range $0 \leq x \leq 10$. The magnetic field decreases the magnitude of Φ . Figure 3 explains the distribution of the thermodynamic temperature θ . In the context of the two theories, in the absence and presence of a magnetic field, θ starts with increasing to a maximum value, then decreases to a minimum value and also moves in the wave propagation. The magnetic field increases the magnitude of θ , then decreases, again increases, and in the last decreases it. Figure 4 explains that the distribution of the stress component σ_{zz} begins from a negative value and satisfies the boundary condition at $x = 0$. In the context of the two theories, in the

absence and presence of a magnetic field, σ_{zz} starts with decreasing to a minimum value, then increases to a maximum value, and also moves in the wave propagation. The magnetic field decreases the magnitude of σ_{zz} , then increases, again decreases, and in the last increases it. Figure 5 depicts the distribution of the stress component σ_{xz} and demonstrates that it reaches a zero value and satisfies the boundary condition at $x = 0$. In the context of the two theories, in the absence and presence of a magnetic field, σ_{xz} starts with increasing to a maximum value, then decreases to a minimum value, and also moves in the wave propagation. The magnetic field increases the magnitude of σ_{xz} , then decreases, again increases, and in the last decreases it. Figure 6 depicts the distribution of the tangential couple stress m_{zy} and demonstrates that it reaches a zero value and satisfies the boundary condition at $x = 0$. In the context of the two theories and in the presence of a magnetic field, m_{zy} starts with increasing to a maximum value, then decreases to a minimum value, and also moves in the wave propagation. However, in the context of the two theories and in the absence of a magnetic field, m_{zy} starts with decreasing to a minimum value, then increases to a maximum value, and also moves in the wave propagation. The magnetic field increases the magnitude of m_{zy} , then decreases, again increases, and so on. Figure 7 describes the distribution of the micro-rotation component Φ_2 . In the context of the two theories and in the presence of a magnetic field, Φ_2 starts with increasing to a maximum value, then decreases to a minimum value, and also moves in the wave propagation. However, in the context of the two theories and in the absence of a magnetic field, Φ_2 starts with decreasing to a minimum value, then increases to a maximum value, and also moves in the wave propagation. The magnetic field increases the magnitude of Φ_2 , then decreases, again increases, and in the last decreases it. Figures 1–7 demonstrate that the values of all the physical quantities converge to zero by increasing the distance z , the behavior of two theories are similar. These trends obey elastic and thermoelastic properties of the solid.

Figures 8–14 show comparisons between the vertical displacement w , the thermodynamic temperature θ , the conductive temperature Φ , the stress components σ_{zz} , σ_{xz} , the tangential couple stress m_{zy} and micro-rotation component Φ_2 for one temperature ($\delta = 0$) and two temperature ($\delta = 2 \times 10^{-14}$) in the presence of a magnetic field ($H_0 = 140$) and an internal heat source ($Q_0 = 5.5$).

Figure 8 explains that the distribution of the vertical displacement w begins from positive values. In the context of the two theories, w starts with decreasing to a minimum value, then increases, and then becomes nearly constant for $\delta = 0$. Figure 9 exhibits the distribution of the conductive temperature Φ and demonstrates that it reaches a zero value and satisfies the boundary condition at $x = 0$. In the context of the two theories, Φ starts with increasing to a maximum value, then decreases

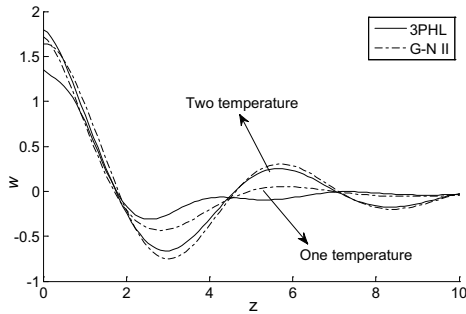


Figure 8: Vertical displacement distribution w for one and two-temperature.

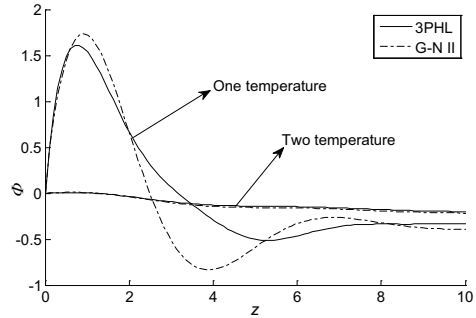


Figure 9: Conductive temperature distribution Φ for one and two-temperature.

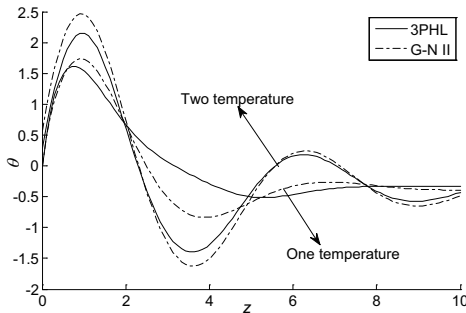


Figure 10: Thermodynamic temperature distribution θ for one and two-temperature.

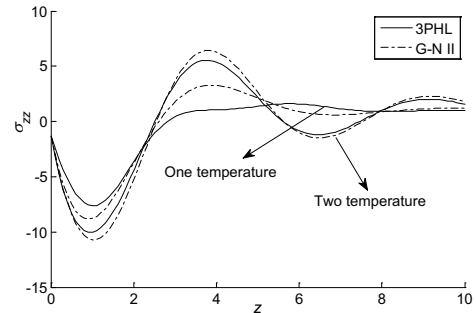


Figure 11: Distribution of the stress component σ_{zz} for one and two-temperature.

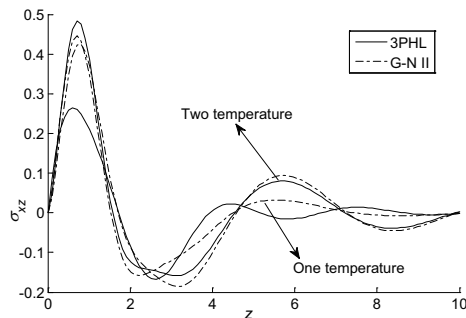


Figure 12: Distribution of the stress component σ_{xz} for one and two-temperature.

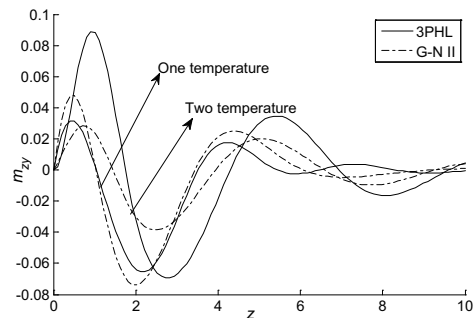


Figure 13: Distribution of the tangential couple stress m_{zy} for one and two-temperature.

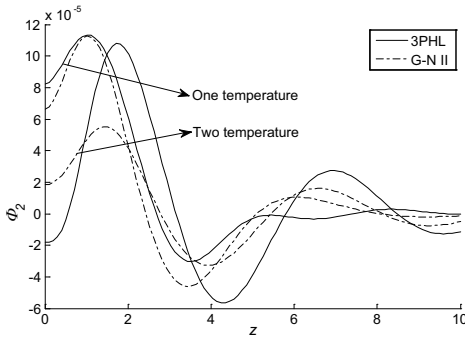


Figure 14: Distribution of the micro-rotation component Φ_2 for one and two-temperature.

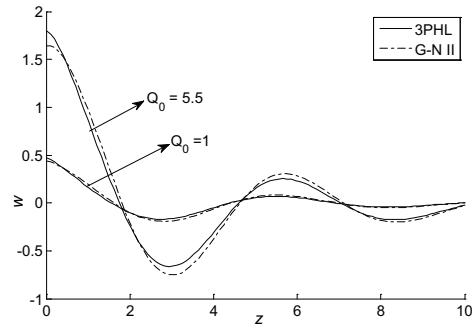


Figure 15: Vertical displacement distribution w for different values of an internal heat source.

to a minimum value, and again increases for $\delta = 0$. Figure 10 exhibits that the distribution of the thermodynamic temperature θ begins from positive values. In the context of the two theories, θ starts with increasing to a maximum value, then decreases to a minimum value, and again increases for $\delta = 0$. Figure 11 explains that the distribution of the stress component σ_{zz} begins from a negative value and satisfies the boundary condition at $x = 0$. In the context of the two theories, σ_{zz} starts with decreasing to a minimum value, then increases, and again decreases for $\delta = 0$. Figure 12 shows the distribution of the stress component σ_{xz} and demonstrates that it reaches a zero value and satisfies the boundary condition at $x = 0$. In the context of the two theories, σ_{xz} starts with increasing to a maximum value, then decreases to a minimum value, and also moves in the wave propagation for $\delta = 0$. Figure 13 depicts the distribution of the tangential couple stress m_{zy} and demonstrates that it reaches a zero value and satisfies the boundary condition at $x = 0$. In the context of the two theories, m_{zy} starts with increasing to a maximum value, then decreases to a minimum value, and also moves in the wave propagation for $\delta = 0$. Figure 14 describes the distribution of the micro-rotation component Φ_2 . In the context of the two theories, Φ_2 starts with increasing to a maximum value, then decreases to a minimum value, and also moves in the wave propagation for $\delta = 0$.

Figures 15–21 show comparisons between the vertical displacement w , the thermodynamic temperature θ , the conductive temperature Φ , the stress components σ_{zz} , σ_{xz} , the tangential couple stress m_{zy} and micro-rotation component Φ_2 for a two-temperature magneto-micropolar medium ($H_0 = 140$, $\delta = 2 \times 10^{-14}$) and for different values of an internal heat source ($Q_0 = 5.5$, $Q_0 = 1$).

Figure 15 explains that the distribution of the vertical displacement w begins from positive values. In the context of the two theories, w starts with decreasing to a

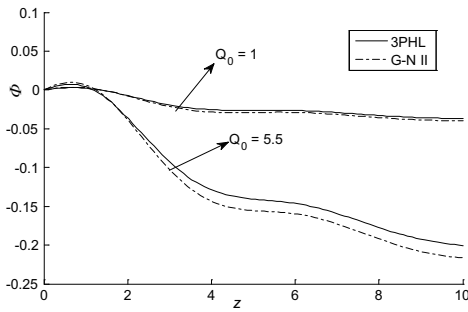


Figure 16: Conductive temperature distribution Φ for different values of an internal heat source.

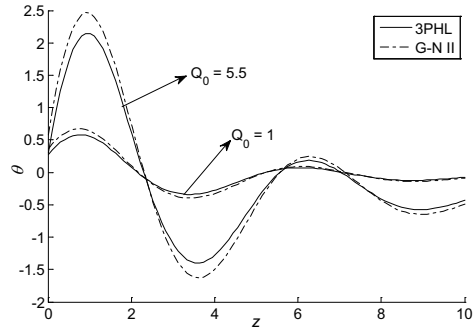


Figure 17: Thermodynamic temperature distribution θ for different values of an internal heat source.

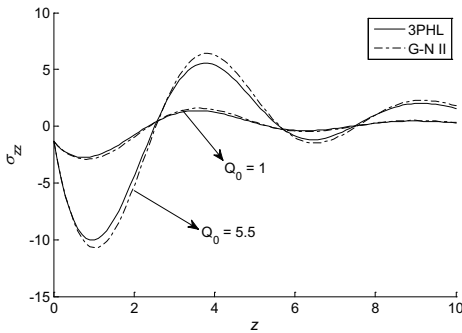


Figure 18: Distribution of the stress component σ_{zz} for different values of an internal heat source.

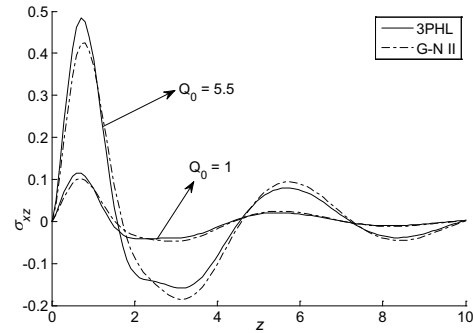


Figure 19: Distribution of the stress component σ_{xz} for different values of an internal heat source.

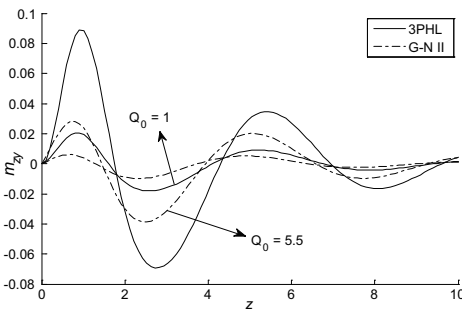


Figure 20: Distribution of the tangential couple stress $m_{z\gamma}$ for different values of an internal heat source.

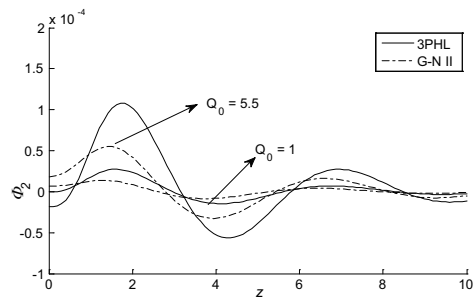


Figure 21: Distribution of the micro-rotation component Φ_2 for different values of an internal heat source.

minimum value, then increases, and again decreases for $Q_0 = 1$. Figure 16 exhibits the distribution of the conductive temperature Φ and demonstrates that it reaches a zero value and satisfies the boundary condition at $x = 0$. In the context of the two theories, Φ decreases in the range $0 \leq x \leq 10$ for $Q_0 = 1$. Figure 17 exhibits that the distribution of the thermodynamic temperature θ begins from positive values. In the context of the two theories, θ starts with increasing to a maximum value, then decreases to a minimum value, and also moves in the wave propagation for $Q_0 = 1$. Figure 18 explains that the distribution of the stress component σ_{zz} begins from a negative value and satisfies the boundary condition at $x = 0$. In the context of the two theories, σ_{zz} starts with decreasing to a minimum value, then increases, and also moves in the wave propagation for $Q_0 = 1$. Figure 19 shows the distribution of the stress component σ_{xz} and demonstrates that it reaches a zero value and satisfies the boundary condition at $x = 0$. In the context of the two theories, σ_{xz} starts with increasing to a maximum value, then decreases to a minimum value, and also moves in the wave propagation for $Q_0 = 1$. Figure 20 depicts the distribution of the tangential couple stress m_{zy} and demonstrates that it reaches a zero value and satisfies the boundary condition at $x = 0$. In the context of the two theories, m_{zy} starts with increasing to a maximum value, then decreases to a minimum value, and also moves in the wave propagation for $Q_0 = 1$. Figure 21 describes the distribution of the micro-rotation component Φ_2 . In the context of the two theories, Φ_2 starts with increasing to a maximum value, then decreases to a minimum value, and also moves in the wave propagation for $Q_0 = 1$.

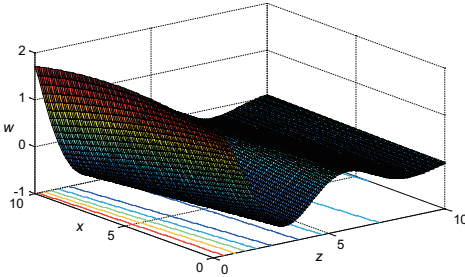


Figure 22: Vertical displacement distribution w based on the 3PHL model.

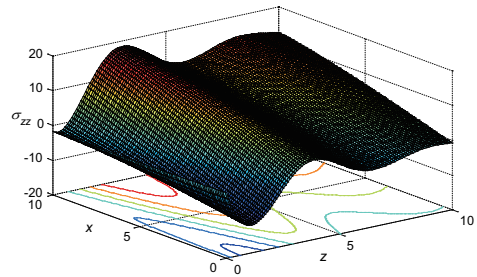


Figure 23: Distribution of the stress component σ_{zz} based on the 3PHL model.

Figures 22–26 are giving 3D surface curves for the physical quantities, i.e., the vertical displacement w , the stress components σ_{zz} , σ_{xz} , the tangential couple stress m_{zy} and micro-rotation component Φ_2 to study the effect of a magnetic field on the wave propagation within a two-temperature micropolar thermoelastic isotropic medium with an internal heat source in the context of the 3PHL model. These figures are very important to study the dependence of these physical quantities on the

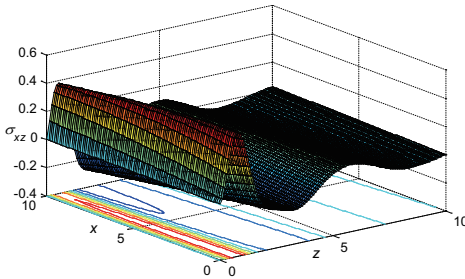


Figure 24: Distribution of the stress component σ_{xz} based on the 3PHL model.

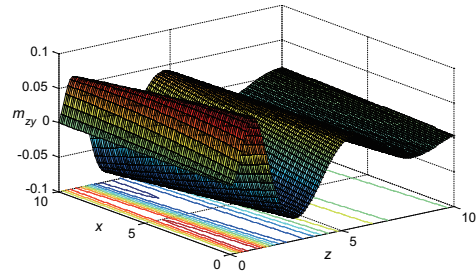


Figure 25: Distribution of the tangential couple stress m_{zy} based on the 3PHL model.

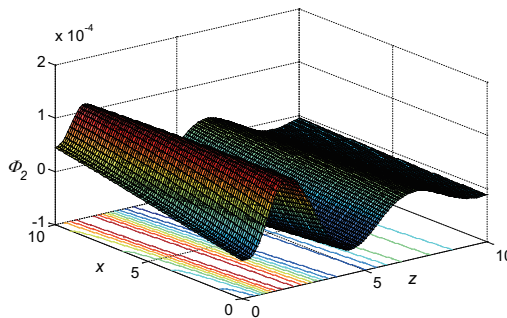


Figure 26: Distribution of the micro-rotation component Φ_2 based on the 3PHL model.

vertical component of distance. The curves obtained are highly depending on the vertical distance from origin, all the physical quantities satisfy boundary condition and are moving in the wave propagation.

7 Concluding remarks

A rigorous mathematical study of thermoelasticity in solid materials has been conducted utilizing two different, robust, well-formulated theories, namely the 3PHL model and the Green-Naghdi theory without dissipation. The cases of a magnetic field presence and absence have been addressed as well as a two-temperature paramter. Analytical solutions based upon normal mode analysis for thermoelasticity in solids have been developed and utilized. The computations have revealed that:

- 1) There are significant differences in the field quantities under the GN-II theory and the 3PHL model due to the phase-lag of temperature gradient and the

phase-lag of heat flux.

- 2) The magnetic field, two-temperature parameter and magnitude of an internal heat source have important roles in the distributions of the field quantities.
- 3) Deformation of a body depends on the nature of the applied force as well as the type of boundary conditions.
- 4) The curves in the context of the 3PHL model and the GN-II theory decrease exponentially with increasing z ; this indicates that the thermoelastic waves are un-attenuated and non-dispersive, while purely thermoelastic waves undergo both attenuation and dispersion.
- 5) The vertical distance plays a significant role on all the physical quantities.

References

Abbas, I. A. (2014): Three-phase-lag model on thermoelastic interaction in an unbounded fiber-reinforced anisotropic medium with a cylindrical cavity. *Journal of Computational and Theoretical Nanoscience*, vol. 11, no. 4, pp. 987–992.

Abbas, I. A.; Zenkour, A. M. (2014): Two-temperature generalized thermoplastic interaction in an infinite fiber-reinforced anisotropic plate containing a circular cavity with two relaxation times. *Journal of Computational and Theoretical Nanoscience*, vol. 11, no. 1, pp. 1–7.

Abbas, I. A.; Zenkour, A. M. (2015): The effect of magnetic field on thermal shock problem for a fiber-reinforced anisotropic half-space using Green-Naghdi's theory. *Journal of Computational and Theoretical Nanoscience*, vol. 12, no. 3, pp. 438–442.

Abbas, I. A.; Kumar, R.; Sharma, K. D.; Garg, S. K. (2015): Deformation due to thermomechanical sources in a homogeneous isotropic micropolar thermoelastic medium with void. *Journal of Computational and Theoretical Nanoscience*, vol. 12, no. 4, pp. 1698–1708.

Chen, P. J.; Gurtin, M. E. (1968a): On a theory of heat conduction involving two temperatures. *Zeitschrift für angewandte Mathematik und Physik*, vol. 19, no. 4, pp. 614–627.

Chen, P. J.; Williams, W. O. (1968b): A note on non simple heat conduction. *Zeitschrift für Angewandte Mathematik und Physik*, vol. 19, no. 6, pp. 969–970.

Chen, P. J.; Gurtin, M. E.; Williams, W. O. (1969): On the thermodynamics of non-simple elastic materials with two-temperatures. *Zeitschrift für angewandte Mathematik und Physik*, vol. 20, no. 1, pp. 107–112.

Chandrasekharaiah, D. S. (1986): Heat flux dependent micropolar thermoelasticity. *International Journal of Engineering Science*, vol. 24, no. 8, pp. 1389–1395.

Choudhuri, S. R. (2007): On a thermoplastic three-phase-lag model. *Journal of Thermal Stresses*, vol. 30, pp. 231–238.

Das, P.; Kanoria, M. (2012): Two-temperature magneto-thermoelastic response in a perfectly conducting medium based on GN-III model. *International Journal of Pure and Applied Mathematics*, vol. 81, no. 2, pp. 199–229.

Eringen, A. C. (1966): Linear theory of micropolar elasticity. *Journal of Mathematics and Mechanics*, vol. 15, no. 6, pp. 909–923.

Eringen, A. C. (1970): *Foundations of micropolar thermoelasticity*. CISM, Springer-Verlag, Berlin.

Green, A. E.; Naghdi, P. M. (1991): A Re-examination of the basic postulate of thermo-mechanics. *Proceedings: Mathematical and Physical Sciences*, vol. 432, no. 1885, pp. 171–194.

Green, A. E.; Naghdi, P. M. (1992): On undamped heat waves in an elastic solid. *Journal of Thermal Stresses*, vol. 15, no. 2, pp. 253–264.

Green, A. E.; Naghdi, P. M. (1993): Thermoelasticity without energy dissipation. *Journal of Elasticity*, vol. 31, no. 3, pp. 189–208.

Hetnarski, R. B.; Ignaczak, J. (1999): Generalized thermoelasticity. *Journal of Thermal Stresses*, vol. 22, no. 4–5, pp. 451–476.

Hetnarski, R. B.; Ignaczak, J. (2000): Nonclassical dynamical thermoelasticity. *International Journal of Solids and Structures*, vol. 37, no. 1, pp. 215–224.

Kar, A.; Kanoria, M. (2009): Generalized thermo-visco-elastic problem of a spherical shell with three-phase-lag effect. *Applied Mathematical Modelling*, vol. 33, no. 8, pp. 3287–3298.

Kumar, R.; Singh, B. (1998): Reflection of plane waves from the flat boundary of a micropolar thermoelastic half space with stretch. *Indian Journal of Pure and Applied Mathematics*, vol. 29, no. 6, pp. 657–669.

Kumar, R. (2000): Wave propagation in micropolar viscoelastic generalized thermoelastic solid. *International Journal of Engineering Science*, vol. 38, no. 12, pp. 1377–1395.

Kumar, R.; Chawla, V.; Abbas, I. A. (2012): Effect of viscosity on wave propagation in anisotropic thermoelastic medium with three-phase-lag model. *Theoretical & Applied Mechanics*, vol. 39, no. 4, pp. 313–341.

- Kumar, A.; Kumar, R.** (2015): A domain of influence theorem for thermoelasticity with three-phase-lag model. *Journal of Thermal Stresses*, vol. 38, no. 7, pp. 744–755.
- Nowacki, W.** (1986): *Theory of Asymmetric Elasticity*. Oxford, Pergamon.
- Othman, M. I. A.; Kumar, R.** (2009): Reflection of magneto-thermoelasticity waves with temperature dependent properties in generalized thermoelasticity. *International Communications in Heat and Mass Transfer*, vol. 36, no. 5, pp. 513–520.
- Othman, M. I. A.; Atwa, S. Y.** (2011): The effect of magnetic field on 2-D problem of generalized thermo-elasticity without energy dissipation. *International Journal of Industrial Mathematics*, vol. 3, no. 3, pp. 213–226.
- Othman, M. I. A.; Lotfy, Kh.; Said, S. M.; Anwar Bég, O.** (2012): Wave propagation in a fiber-reinforced micropolar thermoelastic medium with voids using models. *Journal of Applied Mathematics and Mechanics*, vol. 8, no. 12, pp. 52–69.
- Othman, M. I. A.; Elmaklizi, Y. D.; Said, S. M.** (2013): Generalized thermoelastic medium with temperature dependent properties for different theories under the effect of gravity field. *International Journal of Thermophysics*, vol. 34, no. 3, pp. 521–537.
- Othman, M. I. A.; Abass, I. A.** (2015): Effect of rotation on magneto-thermoelastic homogeneous isotropic hollow cylinder with energy dissipation using finite element method. *Journal of Computational and Theoretical Nanoscience*, vol. 12, no. 9, pp. 2399–2404.
- Quintanilla, R.; Racke, R.** (2008): A note on stability in three-phase-lag heat conduction. *International Journal of Heat and Mass Transfer*, vol. 51, no. 1–2, pp. 24–29.
- Quintanilla, R.** (2009): Spatial behaviour of solutions of the three-phase-lag heat equation. *Applied Mathematics and Computation*, vol. 213, no. 1, pp. 153–162.
- Singh, B.** (2007): Wave propagation in an orthotropic micropolar elastic solid. *International Journal of Solids and Structures*, vol. 44, no. 11–12, pp. 3638–3645.
- Tzou, D. Y.** (1995): A unified approach for heat conduction from macro-to micro-scales. *ASME Journal of Heat Transfer*, vol. 117, no. 1, pp. 8–16.
- Warren, W. E.; Chen, P. J.** (1973): Propagation in the two temperatures theory of thermoelasticity. *Acta Mechanica*, vol. 16, no. 1–2, pp. 21–33.
- Youssef, H. M.** (2005): Theory of two-temperature generalized thermoelasticity. *IMA Journal of Applied Mathematics*, vol. 71, no. 3, pp. 383–390.

Youssef, H. M. (2006): Generalized magneto-thermoelasticity in a conducting medium with variable material properties. *Applied Mathematics and Computation*, vol. 173, no. 2, pp. 822–833.

Zenkour, A. M.; Abouelregal, A. E. (2015): The fractional effects of a two-temperature generalized thermoelastic semi-infinite solid induced by pulsed laser heating. *Archive of Mechanics*, vol. 67, no. 1, pp. 53–73.